© 2014. Published by The Company of Biologists Ltd | Journal of Cell Science (2014) 127, 1840–1853 doi:10.1242/jcs.144550

RESEARCH ARTICLE

Non-muscle Mlck is required for β-catenin- and FoxO1-dependent downregulation of Cldn5 in IL-1β-mediated barrier dysfunction in brain endothelial cells

Richard S. Beard, Jr[1], Ricci J. Haines[2], Kevin Y. Wu[1], Jason J. Reynolds[1], Stephanie M. Davis[1], John E. Elliott[1], Nikolay L. Malinin[1], Victor Chatterjee[1], Byeong J. Cha[1], Mack H. Wu[2] and Sarah Y. Yuan[1,*]

ABSTRACT

Aberrant elevation in the levels of the pro-inflammatory cytokine interleukin-1β (IL-1β) contributes to neuroinflammatory diseases. Blood–brain barrier (BBB) dysfunction is a hallmark phenotype of neuroinflammation. It is known that IL-1β directly induces BBB hyperpermeability but the mechanisms remain unclear. Claudin-5 (Cldn5) is a tight junction protein found at endothelial cell–cell contacts that are crucial for maintaining brain microvascular endothelial cell (BMVEC) integrity. Transcriptional regulation of Cldn5 has been attributed to the transcription factors β-catenin and forkhead box protein O1 (FoxO1), and the signaling molecules regulating their nuclear translocation. Non-muscle myosin light chain kinase (nmMlck, encoded by the *Mylk* gene) is a key regulator involved in endothelial hyperpermeability, and IL-1β has been shown to mediate nmMlck-dependent barrier dysfunction in epithelia. Considering these factors, we tested the hypothesis that nmMlck modulates IL-1β-mediated downregulation of Cldn5 in BMVECs in a manner that depends on transcriptional repression mediated by β-catenin and FoxO1. We found that treating BMVECs with IL-1β induced barrier dysfunction concomitantly with the nuclear translocation of β-catenin and FoxO1 and the repression of Cldn5. Most importantly, using primary BMVECs isolated from mice null for nmMlck, we identified that Cldn5 repression caused by β-catenin and FoxO1 in IL-1β-mediated barrier dysfunction was dependent on nmMlck.

KEY WORDS: Non-muscle myosin light chain kinase, Claudin-5, FoxO1, IL-1β, β-catenin, Blood–brain barrier, Neuroinflammation

INTRODUCTION

Endothelial barrier function is a crucial component of vascular and tissue homeostasis. The barrier function of the endothelium is considered to be selectively permeable rather than completely restrictive, although the degree of endothelial permeability is heterogeneous throughout the vascular tree (Mehta and Malik, 2006; Michel and Curry, 1999). The endothelium of the cerebral microcirculation is considered to be the most restrictive endothelium and is termed the blood–brain barrier (BBB). The highly developed endothelial cell–cell (EC–EC) contacts of the BBB restrict paracellular diffusion, forcing most solute flux across the cerebral endothelium to occur by transcellular routes (Banks, 1999; Miller, 2010). Dysfunction of the BBB, and thus BBB hyperpermeability, has been implicated in the onset and/or progression of several neuroinflammatory diseases, such as traumatic brain injury, stroke, multiple sclerosis, encephalitis and Alzheimer disease (Hawkins and Davis, 2005; Winter et al., 2004; Zlokovic, 2008). Hence, understanding the mechanisms of inflammatory-mediated BBB disruption is of crucial importance.

Aberrant elevation in the levels of the pro-inflammatory cytokine interleukin (IL)-1β has been implicated as a significant mediator of BBB dysfunction in neuroinflammatory diseases. Several lines of evidence from animal studies have supported a role for IL-1β in BBB dysfunction during neuroinflammation: (1) IL-1β concentrations are elevated concomitantly with BBB hyperpermeability in animal models of neuroinflammation (Basu et al., 2004; Chakraborty et al., 2010; Simi et al., 2007); (2) injecting recombinant IL-1β induces BBB hyperpermeability (Blamire et al., 2000; Quagliarello et al., 1991); and (3) IL-1β receptor antagonists, or genetic deletion of the IL-1 receptor, attenuate BBB hyperpermeability that is induced by neuroinflammation (Lazovic et al., 2005; Yamasaki et al., 1995). Furthermore, evidence for IL-1β mediating BBB hyperpermeability is also reinforced by *in vitro* experiments that demonstrate a direct effect of IL-1β in the induction of BBB dysfunction (Didier et al., 2003). We have recently reported that treating primary human brain microvascular endothelial cells (BMVECs) with IL-1β induces PKCθ-dependent barrier dysfunction (Rigor et al., 2012). IL-1β has also been implicated in causing dysfunction of other tissue barriers, such as lung microvascular endothelial cell (LMVEC) permeability in acute lung injury (Ganter et al., 2008) and gut epithelial barrier dysfunction in inflammatory bowel disease (Ligumsky et al., 1990). In contrast to the evidence in favor of a role for IL-1β-mediated vascular permeability in several diseases, there is a relative paucity of information regarding the related molecular mechanisms.

The molecular composition of EC–EC contacts is complex, but consists largely of two distinct junctions known as adherens junctions and tight junctions (reviewed in detail in Dejana, 2004; McEwen et al., 2012). Adherens junctions are commonly expressed in all endothelial cells and, in addition to cell–cell adhesion, play an important role in vascular morphogenesis and remodeling, whereas tight junctions are important for sealing the paracellular gaps and forming the 'barrier' properties of specialized endothelia, such as the BBB (Liebner et al., 2008). Tight junctions consist of the proteins occludin (Ocln) and members of the claudin (Cldn) family that form both homotypic and heterotypic contacts at EC–EC connections, and are linked

[1]Department of Molecular Pharmacology and Physiology, Morsani College of Medicine, University of South Florida, Tampa, FL 33612, USA. [2]Department of Surgery, Morsani College of Medicine, University of South Florida, Tampa, FL 33612, USA.

*Author for correspondence (syuan@health.usf.edu)

Received 11 October 2013; Accepted 12 January 2014

Journal of Cell Science

Journal of Cell Science (2014) 127, 1840–1853 doi:10.1242/jcs.144550

intracellularly to the actin cytoskeleton by zonula occludens proteins (ZO-1 and ZO-2) (Hawkins and Davis, 2005). The precise role of Ocln in tight junctions of the BBB is unknown, and the protein might serve only to strengthen already-existing tight junctions, because Ocln-knockout mice exhibit normal development and maturation of tight junction strands, yet overexpression of Ocln in cells that already express Cldns strengthens barrier properties (Sohet and Daneman, 2013). Of the 24 Cldn isoforms, only Cldns 1, 3, 5 and 12 are expressed in the vascular endothelium (Liebner et al., 2008; Wolburg et al., 2003). Even though several Cldn isoforms are expressed in both epithelial and endothelial tight junctions, Cldn5 is the only isoform that is exclusively found in endothelium (Hawkins and Davis, 2005). Although Cldn5 is pan-endothelial, its expression is highest in the brain, and the degree of Cldn5 expression is positively correlated with junction 'tightness' (Daneman et al., 2010). Furthermore, Cldn5 downregulation has been associated with increased BBB permeability in animal models of neuroinflammation and neurodegeneration (Beard et al., 2011; McColl et al., 2008). However, the mechanisms of Cldn5 regulation in pathologic conditions are still not entirely understood.

Recently, a mechanism for β-catenin-dependent regulation of Cldn5 during endothelial development was discovered, whereby β-catenin is sequestered at adherens junctions upon EC–EC contact, thus preventing the nuclear accumulation of β-catenin and the resulting transcriptional repression of the *Cldn5* gene (Taddei et al., 2008). In subconfluent endothelial cells, β-catenin localizes with the forkhead box transcription factor (FoxO1) and inhibits TCF/LEF-dependent transcription of *Cldn5*. When cells reach confluence, β-catenin is sequestered by vascular endothelial (VE)-cadherin at adherens junctions, whereas FoxO1 is phosphorylated by constitutively active Akt, reducing FoxO1 nuclear localization. This and other mechanisms for the upregulation of tight junctions have been explored mainly in the developing endothelium as opposed to in mature endothelium responding to external stimuli. Evidence is emerging that this mechanism for Cldn5 regulation can be reversed in response to pathologic stimuli, such as in hyperhomocysteinemia (Beard et al., 2011) and acrolein-induced acute lung injury (Jang et al., 2011). In addition, it has been demonstrated that IL-1β signaling leads to downregulation of Cldn5 expression at the BBB, particularly after mild ischemic brain injury in mice (McColl et al., 2008). Considering the role of β-catenin activation, nuclear translocation and β-catenin-mediated repression of the *Cldn5* gene in the response to pathologic stimuli, it would be valuable to determine whether this mechanism is present in IL-1β-mediated BMVEC barrier dysfunction, and to investigate potential regulators of this pathway. Such information could be important for determining therapeutic targets for BBB dysfunction in neuroinflammatory conditions.

Myosin light chain kinase (Mylk or Mlck) has been shown to act as a crucial regulator of endothelial permeability. Mlck is a calcium/calmodulin-dependent kinase that is known to phosphorylate myosin regulatory chains (MLC) and promote the interaction of myosin with actin during contractile activity. Of the four major isoforms encoded by the *Mylk* gene, two (Mlck1 and Mlck2) are expressed in endothelial cells. Mlck1, or non-muscle Mlck (nmMlck, 210 kDa), represents a unique isoform expressed in mature endothelium (Yuan and Rigor, 2010). Experiments using genetically modified animals have demonstrated the significance of nmMlck in mediating endothelial contractility and hyperpermeability under pro-inflammatory conditions. Importantly, nmMlck-isoform-specific knockout ($nmmlck^{-/-}$) mice demonstrate a phenotype devoid of cardiovascular defects, yet these mice display an attenuated vascular inflammatory response to acute lung injury (Wainwright et al., 2003), severe burns (Reynoso et al., 2007), atherosclerosis (Sun et al., 2011) and improved survival in endotoxic shock (Ranaivo et al., 2007). Although the role of nmMlck in mediating both the opening of endothelial cell–cell junctions and the paracellular hyperpermeability response to proinflammatory agents (including histamine, thrombin, ROS and activated neutrophils) has been well documented (reviewed in Yuan and Rigor, 2010), the role of nmMlck in IL-1β-mediated dysfunction of the BBB has not been investigated. Because nmMlck has been shown to be involved in dissociating β-catenin from VE-cadherin at the adherens junction (Sun et al., 2011), in this study, we hypothesized that nmMlck modulates IL-1β-mediated downregulation of Cldn5 and dysfunction of the BMVEC barrier in a manner that involves β-catenin activation, nuclear translocation and repression of the *Cldn5* gene (Fig. 1).

RESULTS

IL-1β induces Cldn5 downregulation and size-selective hyperpermeability in brain microvascular endothelial cell monolayers

We and others have shown that treating cultured BMVECs with IL-1β induces endothelial barrier dysfunction (Didier et al., 2003; Rigor et al., 2012). In this first set of experiments, using immortalized BMVECs (bEnd.3 cells), we extend this observation and further characterize the mechanisms underlying BMVEC barrier dysfunction that is associated with aberrant IL-1β signaling. First, we analyzed transendothelial electrical resistance (TER) in our model, by growing bEnd.3 cells to confluence, allowing them to mature for 5 days post confluence and then treating them for 24 hours with IL-1β while measuring cell–cell adhesive resistance to electrical current using an electric cell–substrate impedance sensing (ECIS) system (Fig. 2A,B). Consistent with reports in other endothelial models (Rigor et al., 2012), TER responses began to drop in a dose- and time-dependent manner within the first 6 hours of treatment with IL-1β. Furthermore, we identified that IL-1β-mediated decreases in TER continued beyond 6 hours and persisted for at least 24 hours after stimulation.

TER measures the 'tightness' of cell–cell adhesion (i.e. paracellular resistance), but only to electric current. TER does not indicate the permeability of the monolayer to molecules of different sizes. Therefore, using transwell permeability assays, we measured the permeability coefficient (P_S) for differently sized molecules in bEnd.3 monolayers that were treated with IL-1β for 24 hours, and compared the results with those of untreated monolayers. Treatment with IL-1β caused a time-dependent increase in the permeability of the monolayer to sodium fluorescein (~0.4 kDa) that was inversely correlated with the IL-1β-mediated TER changes (Fig. 2C). Additionally, when comparing differently sized molecules, we found that IL-1β induced a significant increase in the permeability of bEnd.3 monolayers to sodium fluorescein and TRITC–dextran (4.4 kDa), but not to FITC–albumin (66.4 kDa), suggesting that IL-1β mediates size-selective hyperpermeability (Fig. 2D).

There is a growing body of evidence showing that Cldn5 is the predominant molecular target in neuroinflammation-induced disruption of the BBB (McColl et al., 2008). Furthermore,

Journal of Cell Science (2014) 127, 1840–1853 doi:10.1242/jcs.144550

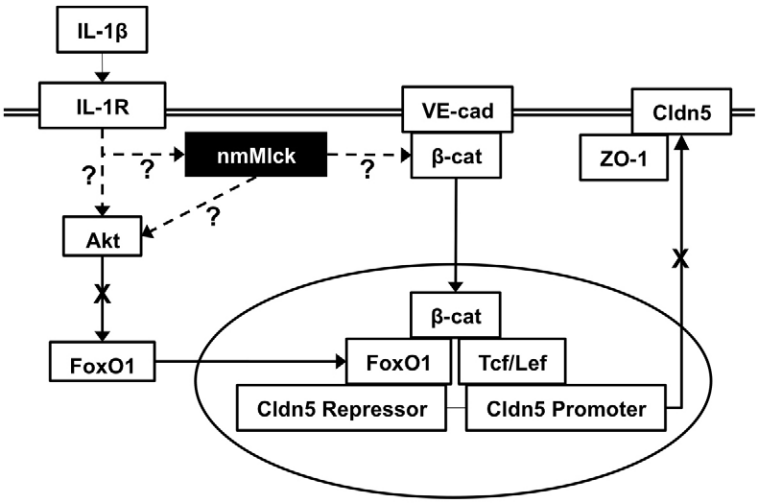

Fig. 1. Diagram of signaling pathways through which non-muscle myosin light chain kinase (nmMlck) might be involved in IL-1β-mediated BMVEC barrier dysfunction. We hypothesize that nmMlck modulates IL-1β-mediated downregulation of Cldn5 and dysfunction of the BMVEC barrier in a manner that promotes the nuclear translocation of β-catenin and the repression of the Cldn5 gene. Question marks and dashed lines indicate unknown signaling mechanisms, whereas solid lines indicate previously established mechanisms.

Cldn5-deficient mice exhibit size-selective 'loosening' of the BBB and die several hours postpartum (Nitta et al., 2003). Therefore, we examined Cldn5 expression and localization in response to IL-1β treatment by using western blotting, confocal immunofluorescence analysis, in-cell western (ICW) assays and quantitative RT-PCR. Confocal microscopy revealed that, in

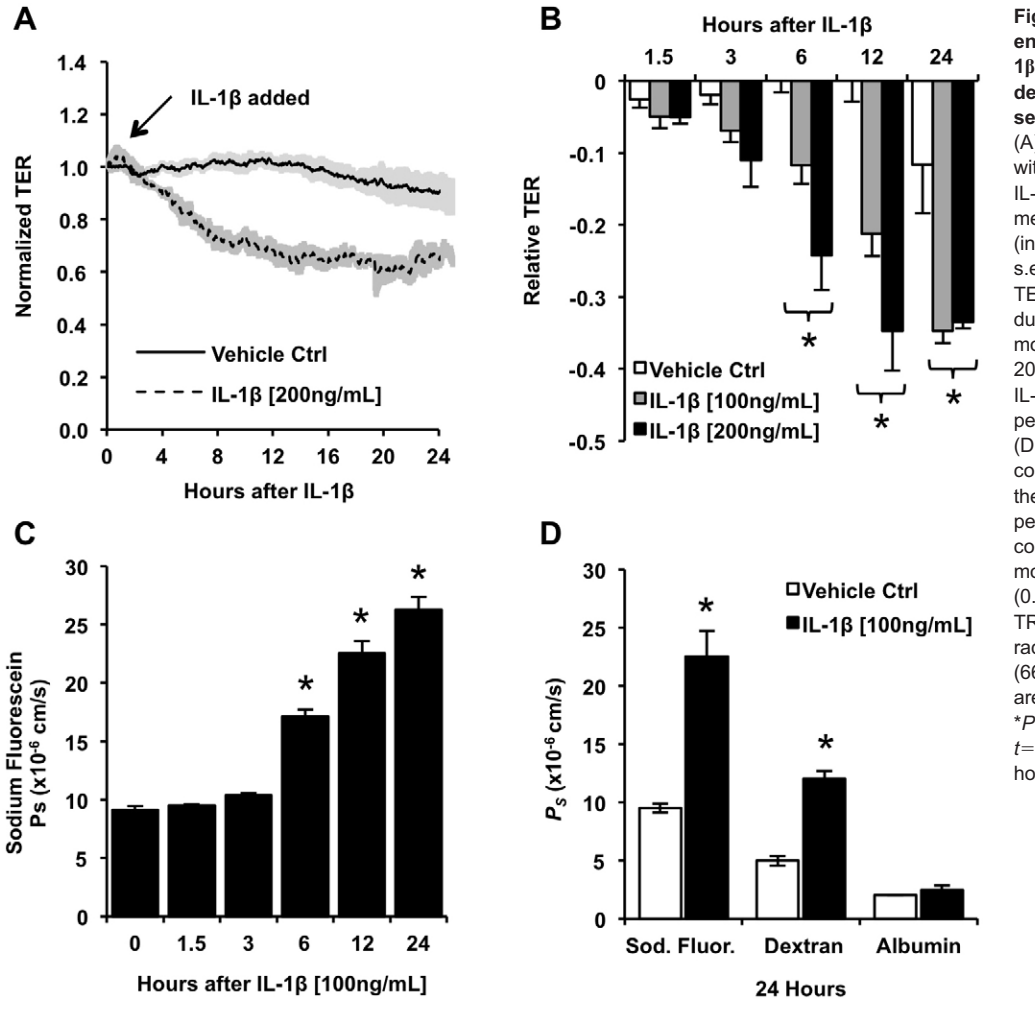

Fig. 2. Treating brain microvascular endothelial cells (bEnd.3 cells) with IL-1β induces a time- and dose-dependent decrease in TER while increasing size-selective monolayer permeability. (A) ECIS tracings of monolayers treated with vehicle control (0.1% BSA in PBS) or IL-1β (200 ng/ml). Tracings indicate the mean resistance normalized to $t=0$ (indicated by arrow) and shading indicates s.e.m. (B) Statistical analysis of relative TER decline at the indicated time points during the treatment of bEnd.3 monolayers with IL-1β (either 100 or 200 ng/ml). (C) Time-course of the IL-1β-mediated increase in monolayer permeability to sodium fluorescein. (D) Monolayers were treated with vehicle control or IL-1β (100 ng/ml) for 24 hours, then transwell permeability assays were performed to determine permeability coefficients (P_S) for the following molecules: sodium fluorescein (0.376 kDa; Stokes' radius≈0.45 nm), TRITC–dextran (4.4 kDa; Stokes' radius≈1.4 nm) and FITC–albumin (66.4 kDa; Stokes' radius≈3.48 nm). Data are presented as the mean±s.e.m. *$P<0.05$ compared with vehicle control or $t=0$; one-way ANOVA with Dunnett's post hoc analysis.

Journal of Cell Science (2014) 127, 1840–1853 doi:10.1242/jcs.144550

control bEnd.3 cell monolayers, Cldn5 protein was localized to EC–EC junctions and strongly colocalized with the tight junction protein ZO-1 (Fig. 3A, upper panels). However, Cldn5 expression and localization at tight junctions was significantly reduced in monolayers treated with IL-1β (Fig. 3A, lower panels). Additionally, western blot analysis of whole-cell lysates confirmed a significant reduction in Cldn5 levels in response to IL-1β treatment for 24 hours (Fig. 3B). To determine the time-course of IL-1β-mediated downregulation of Cldn5, and whether Cldn5 downregulation correlated with IL-1β-induced barrier dysfunction, we used ICW assays to quantify total Cldn5 expression (Fig. 3C). Cldn5 expression was decreased in a time-dependent manner, and this decrease in expression reached statistical significance after 6 hours of IL-1β treatment. This decrease was correlated with IL-1β-mediated barrier dysfunction and hyperpermeability. In order to discern whether Cldn5 downregulation was the result of altered protein synthesis or degradation, *Cldn5* mRNA levels were assessed at various time-points from 1.5 to 24 hours post-treatment with IL-1β (Fig. 3D). Quantitative RT-PCR analysis revealed that there was a significant decrease in *Cldn5* mRNA levels that preceded the onset of Cldn5 protein changes in response to IL-1β, suggesting that Cldn5 downregulation was the result of a targeted gene regulatory event. Although there is a strong temporal association between IL-1β-mediated barrier dysfunction and Cldn5 downregulation, this data remains largely correlative. Therefore, we used *Cldn5*-specific siRNA to reduce the levels of Cldn5, and compared the permeability coefficients for sodium fluorescein, TRITC–dextran, and FITC–albumin between scrambled controls and Cldn5-deficient monolayers with or without IL-1β treatment (Fig. 3E,F). Indeed, Cldn5-deficient monolayers showed a significant increase in the permeability of the monolayer to 0.4-kDa sodium fluorescein and 4.4-kDa TRITC–dextran, but not to 66.4-kDa FITC–albumin, suggesting that Cldn5 is needed at cell–cell junctions in BMVECs to reduce the paracellular permeability to small molecules. Interestingly, treating Cldn5-deficient monolayers with IL-1β further increased their permeability to sodium fluorescein and TRITC–dextran, whereas their permeability to FITC–albumin remained unchanged.

Transcriptional regulation by FoxO1 and β-catenin mediates IL-1β-induced gene repression of *Cldn5*

Previous reports have identified that the regulation of the *Cldn5* gene in response to pathologic stimuli can be modulated by the binding of FoxO1 to a repressor region in the *Cldn5* promoter, a process which is dependent upon the presence of activated β-catenin to stabilize this repression (Taddei et al., 2008). In mature brain endothelia, constitutively active Akt (pT308 Akt) phosphorylates FoxO1 at threonine 24 (pT24 FoxO1) to prevent its nuclear translocation, and VE-cadherin sequesters β-catenin to prevent its nuclear translocation (Taddei et al., 2008). Therefore, we sought to analyze the effect of IL-1β on Akt–FoxO1 signaling, activation of β-catenin, and the nuclear translocation and binding of both FoxO1 and β-catenin to the *Cldn5* repressor at the earliest time-point post-treatment with IL-1β at which we detected a decrease in *Cldn5* mRNA levels (1.5 hours).

Here, by using western blotting and ICW assays, we identified that a 1.5-hour treatment with IL-1β mediated a decrease in pT308 Akt and pT24 FoxO1 levels (Fig. 4A,B). Furthermore, by using nuclear fractionation and confocal immunofluorescent analysis, we determined that there was an increase in FoxO1 nuclear accumulation (Fig. 4C,E) as a result of IL-1β treatment. Additionally, RT-PCR analysis of known transcriptional targets of FoxO1 (*Cdkn1a* and *Pdk4*) demonstrated that the FoxO1 that accumulated in the nucleus in response to IL-1β treatment was active in the transcriptional regulation of target genes (Fig. 4D). These results suggest that the IL-1β-mediated downregulation of Cldn5 occurs concomitantly with decreased Akt activity and increased nuclear translocation of active FoxO1.

β-catenin is thought to play a dual role in modulating the function of the endothelial barrier, depending on its cellular localization. At the adherens junctions, β-catenin stabilizes VE-cadherin-mediated cell–cell adhesion by anchoring the cytoplasmic tail of VE-cadherin to the actin cytoskeleton. Certain stimuli are known to activate β-catenin, which involves the dissociation of β-catenin from the adherens junction, phosphorylation-mediated stabilization to prevent degradation, and translocation of β-catenin to the nucleus, where it acts as a transcriptional coregulator. Using a co-immunoprecipitation protocol, we found a decrease in the co-precipitation of β-catenin with VE-cadherin after 1.5 hours of stimulating bEnd.3 monolayers with IL-1β (Fig. 5A), a result that indicated a reduced association of β-catenin with adherens junctions. Furthermore, there was an increase in the amount of active β-catenin (clone 8E7), as determined by western blot analysis of whole-cell lysates with an antibody against active β-catenin (Fig. 5B). Both western blotting of nuclear extracts and immunocytochemistry experiments revealed that stimulating bEnd.3 monolayers with IL-1β increased the nuclear localization of β-catenin (Fig. 5C,E). A recent report identified that Wnt signaling in brain endothelia leads to the accumulation of β-catenin in the nucleus, where it might target several genes associated with tight junctions (Liebner et al., 2008). However, in that study, no changes in *Cldn5* expression were reported – Wnt-mediated nuclear accumulation of β-catenin was, instead, only associated with an increase in *Cldn3* expression and a decrease in the expression of plasmalemmal vesicle-associated protein (*Plvap*). Therefore, we ran an RT-PCR array of the same target genes in bEnd.3 cells treated with IL-1β (Fig. 5D). Although there was a mean increase in *Cldn1* expression it did not reach statistical significance. The only genes that were significantly altered in our model were *Cldn5* and *Ocln*.

Given that we found an increase in FoxO1 and β-catenin nuclear translocation, and a decrease in the level of *Cldn5* mRNA in response to IL-1β, we performed chromatin immunoprecipitation (ChIP) assays to determine whether FoxO1 and β-catenin associate with the putative *Cldn5* repressor in response to treatment with IL-1β (Fig. 6). After a 1.5-hour treatment with IL-1β, both FoxO1 and β-catenin immunoprecipitated with the putative *Cldn5* repressor, as determined by both qualitative (Fig. 6A,C) and quantitative (Fig. 6B,D) PCR results. Furthermore, the knockdown of either FoxO1 or β-catenin (Fig. 6E) attenuated both the IL-1β-induced downregulation of *Cldn5* mRNA at 1.5 hours after treatment (Fig. 6F) and barrier dysfunction at 24 hours (Fig. 6G). Collectively, these results suggest that IL-1β-mediated Cldn5 downregulation involves repression of *Cldn5* transcription that is mediated by both β-catenin and FoxO1.

The β-catenin activation elicited by IL-1β-mediated barrier dysfunction is dependent on nmMlck

Several lines of evidence have implicated nmMlck as an important kinase in transducing pro-inflammatory or hyperpermeability signals in the endothelium. Furthermore, IL-1β has been shown to induce dysfunction of the gut barrier through nmMlck in intestinal epithelium (Ma et al., 2005). However, the role of nmMlck in BMVECs or in IL-1β-mediated dysfunction of the

Journal of Cell Science (2014) 127, 1840–1853 doi:10.1242/jcs.144550

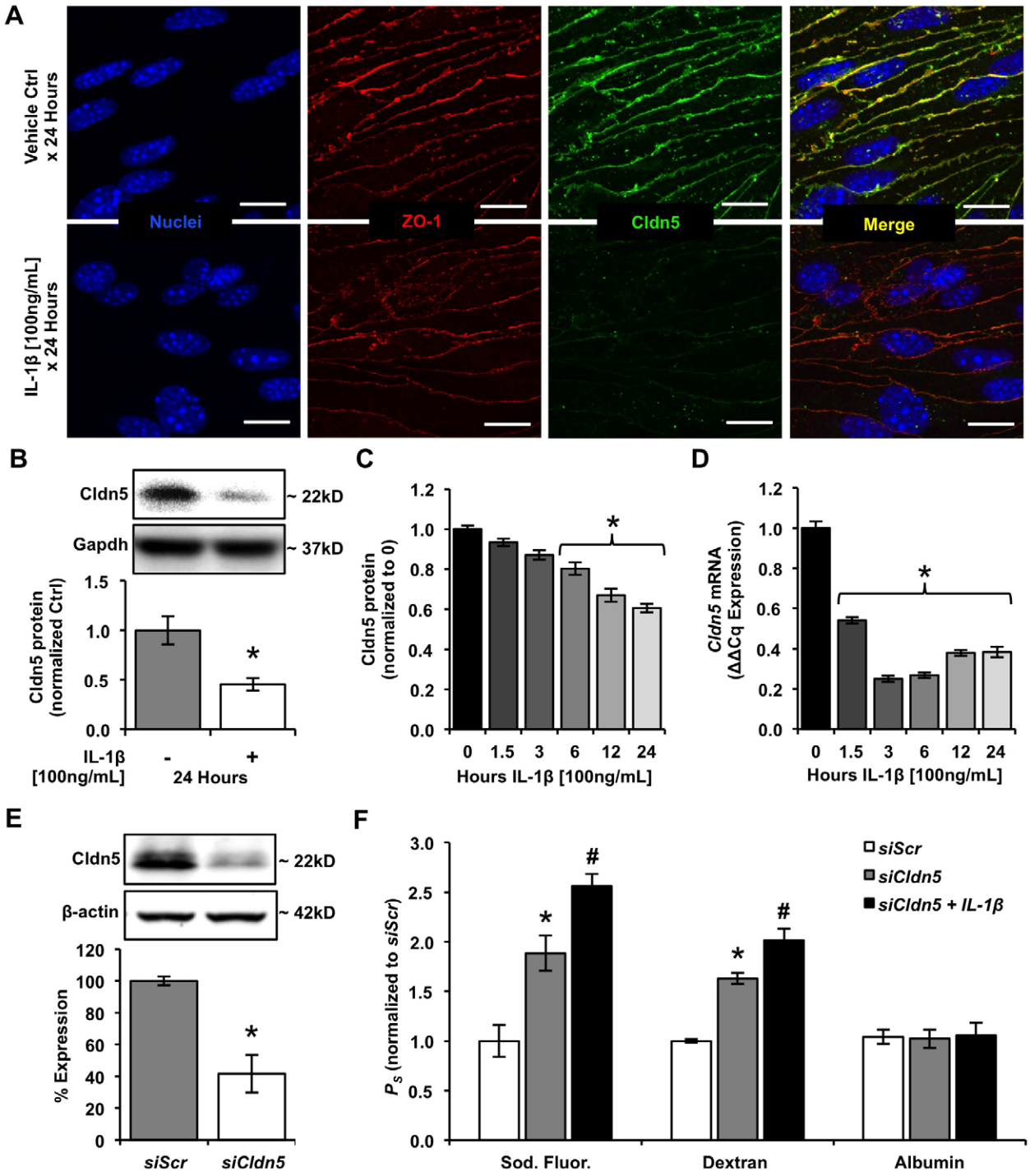

Fig. 3. IL-1β decreases Cldn5 expression in bEnd.3 cells in a manner consistent with IL-1β-mediated barrier dysfunction. (A) Confocal immunofluorescence analysis of the tight junction proteins Cldn5 and zonula occludens-1 (ZO-1) after a 24-hour treatment with IL-1β (100 ng/ml), compared with vehicle control. Scale bars: 20 μm. Cldn5 and ZO-1 are colocalized at cell–cell contacts in vehicle-control-treated cells. In IL-1β-treated cells, no obvious expression or localization changes were observed for ZO-1; however, IL-1β induced a significant reduction in Cldn5 expression at cell–cell contacts. (B) Western blotting for Cldn5 in cell lysates demonstrated that treatment with IL-1β (100 ng/ml) induced ~2-fold decrease in total Cldn5 protein expression. (C) ICWs were used to determine the time-course for the IL-1β-mediated decrease in Cldn5 protein expression. (D) Real-time PCR results demonstrate that IL-1β induced downregulation of *Cldn5* mRNA that preceded the IL-1β-mediated decrease in Cldn5 protein expression. (E) Western blotting providing confirmation and quantification of Cldn5 knockdown that was obtained by treatment with targeted siRNA (*siCldn5*) or scrambled siRNA (*siScr*). (F) Permeability coefficients (P_S) for sodium fluorescein, TRITC-dextran and FITC-albumin were measured in Cldn5-deficient BMVEC monolayers (*siCldn5*) with or without IL-1β (100 ng/ml) treatment for 24 hours, and were compared with those of *siScr* monolayers. Similar to IL-1β treatment, Cldn5 deficiency increased the permeability of the monolayer to sodium fluorescein and TRITC–dextran, but not to FITC–albumin. Moreover, treating Cldn5-deficient monolayers with IL-1β further increased the permeability of the monolayer to sodium fluorescein and TRITC–dextran, whereas FITC–albumin permeability remained unchanged. Data are presented as the mean±s.e.m. *$P<0.05$ compared with the vehicle control, the $t=0$ time-point or *siScr*; #$P<0.05$ compared with *siCldn5* alone; Student's *t*-test or one-way ANOVA with Dunnett's (C,D) and Tukey's (F) post hoc analysis.

Journal of Cell Science (2014) 127, 1840–1853 doi:10.1242/jcs.144550

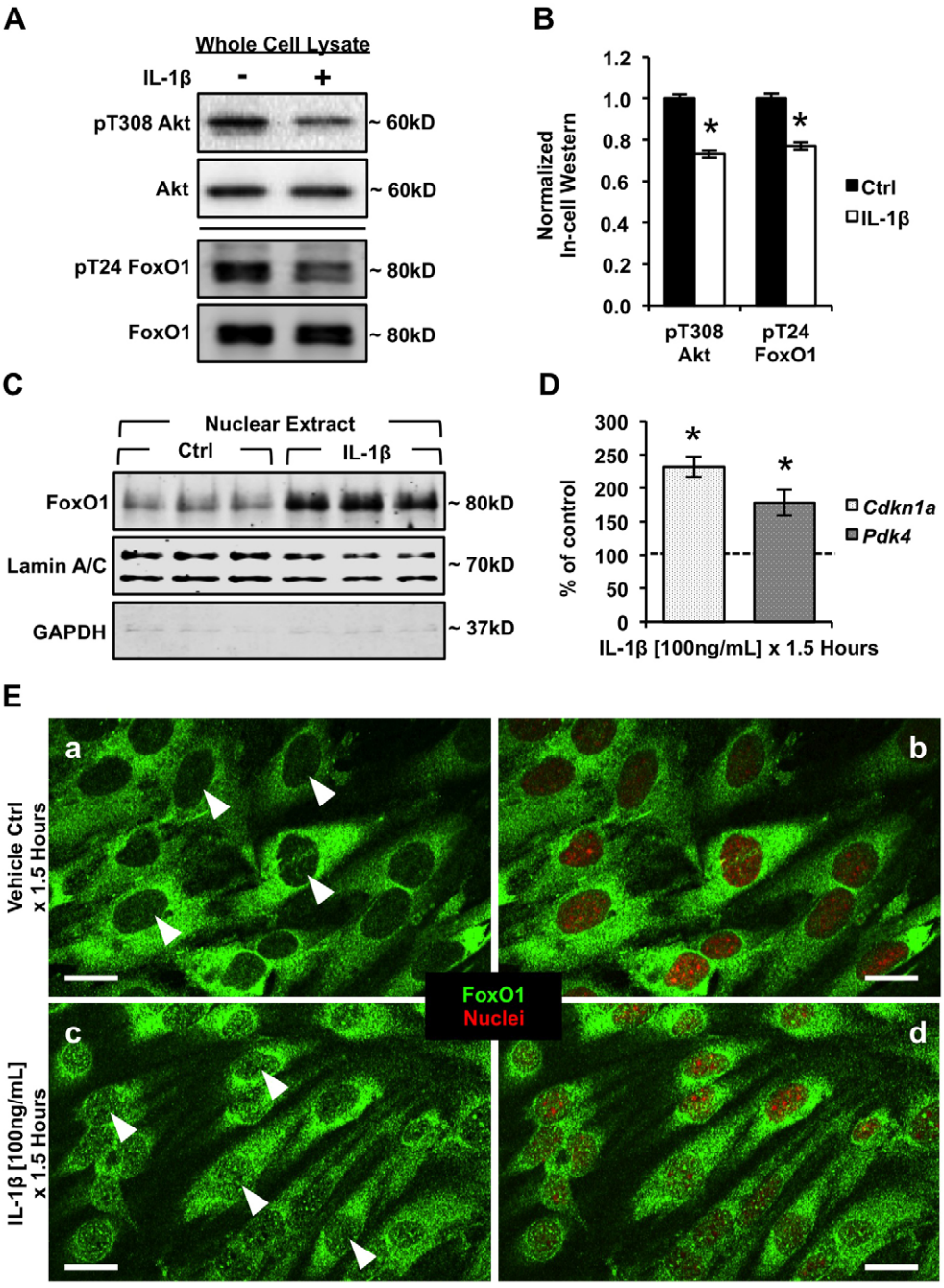

Fig. 4. IL-1β treatment is associated with Akt inactivation, resulting in FoxO1 nuclear accumulation and FoxO1-dependent regulation of gene expression. (A) Representative western blots demonstrate that IL-1β (100 ng/ml for 1.5 hours) inactivated Akt, as indicated by a decrease in phosphorylation of T308. Consistent with inactivation of Akt, IL-1β treatment also led to decreased phosphorylation of FoxO1 on T24. (B) ICWs were used to quantify IL-1β-mediated dephosphorylation of Akt and FoxO1. (C) Western blot analysis of nuclear lysates demonstrated a significant increase in the nuclear accumulation of FoxO1 in response to IL-1β treatment. Lamin A/C was used as a loading control and Gapdh was used to determine the efficacy of nuclear fractionation. (D) Real-time PCR results showed upregulation of two known FoxO1 transcriptional targets, *Cdkn1a* and *Pdk4*. Data are presented as the mean±s.e.m. **P*<0.05 compared with vehicle control; Student's *t*-test. (E) Confocal immunofluorescence analysis revealed an increased nuclear accumulation of FoxO1 in response to IL-1β treatment (c,d) compared with cells treated with vehicle control (a,b). Arrowheads represent the location of nuclei in images without nuclear staining. Scale bars: 20 μm.

endothelial barrier is poorly understood. Considering the role of nmMlck in the instability of adherens junctions, as well as the observed adherens junction instability after IL-1β treatment, we hypothesized that the nuclear accumulation of β-catenin might be the result of nmMlck activity in response to IL-1β. Therefore, by using primary BMVECs from *nmmlck*$^{+/+}$ and *nmmlck*$^{-/-}$ mice (supplementary material Fig. S1), we investigated the role of nmMlck in the IL-1β-mediated downregulation of Cldn5.

After isolating and culturing primary BMVECs, we first determined the effect of IL-1β on nmMlck activation in these cells. Treating BMVECs with IL-1β (100 ng/ml) acutely activated nmMlck (within 15 minutes), as indicated by the increased phosphorylation of tyrosine 464 (Y464) in a time-dependent manner (Fig. 7A). Given that IL-1β-mediated nmMlck activation occurred immediately and persisted for 2 hours after treatment, we next aimed to determine the role of nmMlck in the FoxO1- and β-catenin-dependent processes that were discussed above. ICWs were used to assess IL-1β-mediated inactivation of the Akt–FoxO1 pathway in BMVECs (Fig. 7B). IL-1β decreased the levels of pT308 Akt and pT24 FoxO1 (without changing total protein expression; supplementary material Fig. S2) in BMVECs isolated from both *nmmlck*$^{+/+}$ and *nmmlck*$^{-/-}$ mice, suggesting that nmMlck is not required for IL-1β-mediated Akt inactivation. However, western blotting for active β-catenin and total β-catenin revealed that IL-1β increased the ratio of active β-catenin to total β-catenin in BMVECs isolated from *nmmlck*$^{+/+}$ mice, but not in those isolated from *nmmlck*$^{-/-}$ mice (Fig. 7C), suggesting that nmMlck acts upstream of β-catenin activation. As expected, nmMlck deficiency attenuated IL-1β-mediated β-catenin nuclear accumulation, but not FoxO1 nuclear accumulation (Fig. 7D,E).

Journal of Cell Science (2014) 127, 1840–1853 doi:10.1242/jcs.144550

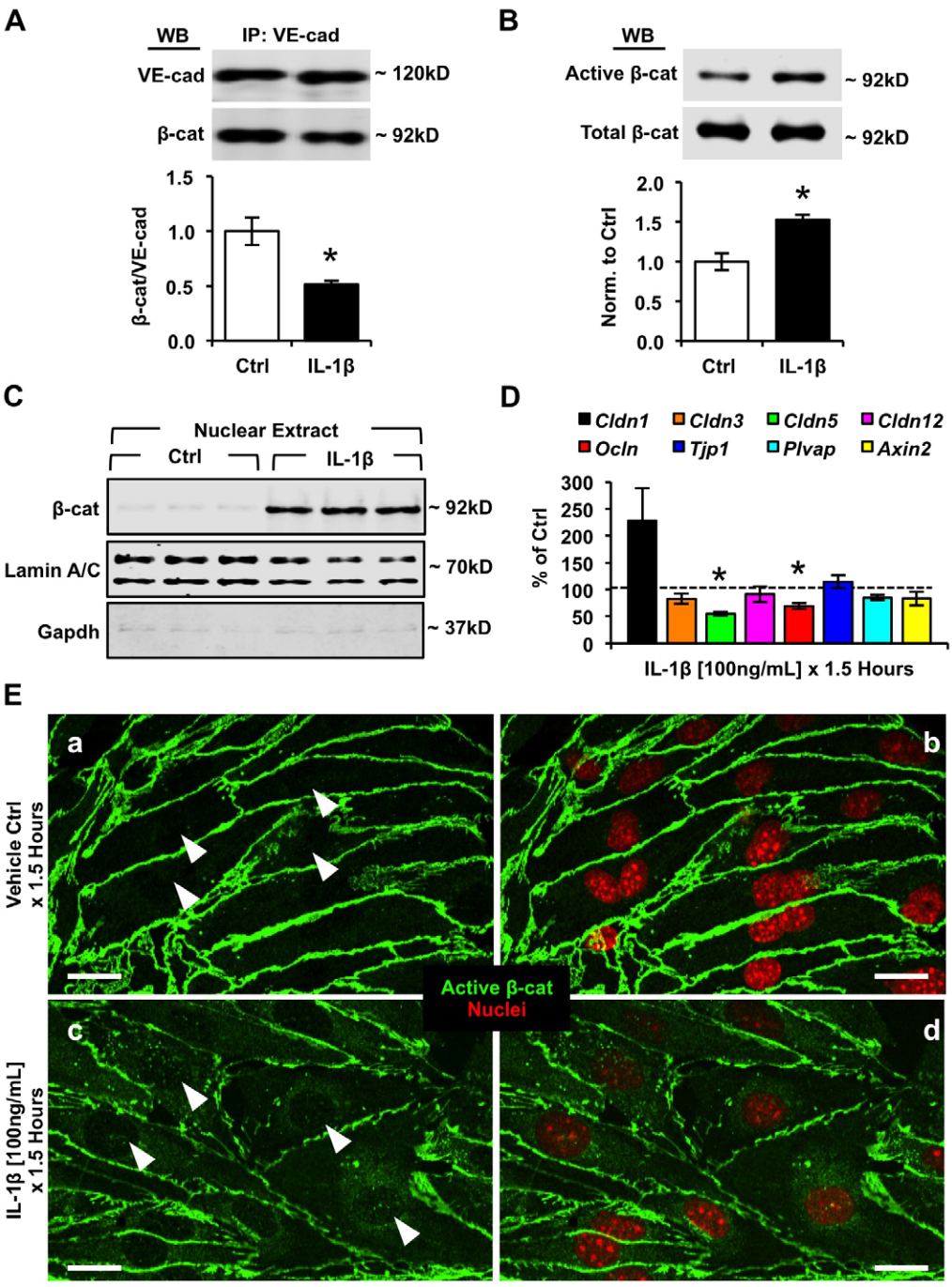

Fig. 5. Treatment of bEnd.3 cells with IL-1β leads to uncoupling of the VE-cadherin–β-catenin complex, an increase in the pool of active β-catenin, and nuclear localization of β-catenin. (A) Co-immunoprecipitation experiments demonstrated that there was a decrease in the amount of β-catenin (β-cat) that precipitated with VE-cadherin (VE-cad) after IL-1β treatment (100 ng/ml, 1.5 hours). (B) Western blotting for active β-catenin (clone 8E7) demonstrated an increase in active β-catenin immunolabeling after IL-1β treatment. Data represent the mean±s.e.m. (C) Western blot analysis of the nuclear fraction showed a significant increase in nuclear accumulation of β-catenin in response to IL-1β treatment. Lamin A/C was used as a loading control, and Gapdh was used to determine the efficacy of nuclear fractionation. The control blots showing Lamin A/C and Gapdh are duplicates of the controls shown in Fig. 4C, as these experiments were performed on the same nuclear extracts and western blots. (D) mRNA levels were determined for *Cldn1*, *Cldn3*, *Cldn5*, *Cldn12*, *Ocln*, *Tjp1*, *Plvap* and *Axin2* from bEnd.3 cells that were treated with IL-1β. Data represent mean mRNA levels (±s.e.m.), shown as a percentage of vehicle control. *$P<0.05$ compared with vehicle control; Student's *t*-test. (E) Confocal immunocytochemistry demonstrates increased nuclear accumulation of β-catenin in response to IL-1β treatment (c without nuclei staining, d with nuclei staining) compared with vehicle control (a without nuclei staining, b with nuclei staining). Arrowheads represent the location of nuclei in images without nuclei staining. Scale bars: 20 μm.

To determine the impact of nmMlck signaling on β-catenin- and FoxO1-dependent transcriptional repression of *Cldn5*, ChIP assays were repeated in BMVECs (Fig. 7F). Although treatment with IL-1β led to nuclear accumulation of FoxO1 in both *nmmlck*$^{+/+}$ and *nmmlck*$^{-/-}$ BMVECs, the absence of β-catenin in the nuclei of IL-1β-treated *nmmlck*$^{-/-}$ BMVECs prevented the binding of FoxO1 to the *Cldn5* repressor. These results suggest that IL-1β-induced nmMlck signaling alters the transcriptional repressive activities of both β-catenin and FoxO1.

In culmination, we confirmed the connection between the nmMlck-dependent molecular mechanisms induced by IL-1β after 1.5 hours of treatment and the IL-1β-mediated barrier dysfunction that is observed after treatment for 24 hours. Western blotting for Cldn5 in lysates obtained from *nmmlck*$^{+/+}$ versus *nmmlck*$^{-/-}$ BMVECs that were cultured with or without IL-1β (100 ng/ml for 24 hours) demonstrated that BMVECs from *nmmlck*$^{+/+}$ mice responded to IL-1β in a similar fashion to bEnd.3 cells. However, nmMlck deficiency in BMVECs rescued IL-1β-mediated Cldn5 downregulation (Fig. 8A). TER measurements were obtained from *nmmlck*$^{+/+}$ versus *nmmlck*$^{-/-}$ BMVECs that were cultured with or without IL-1β (Fig. 8B). Although, on average, bEnd.3 monolayers had higher basal TER levels than BMVECs (data not shown), both bEnd.3 and BMVECs showed the same pattern of response to IL-1β. Namely, *nmmlck*$^{+/+}$ monolayers that were treated with IL-1β displayed a gradual decrease in TER that persisted for at least 24 hours. However,

Journal of Cell Science (2014) 127, 1840–1853 doi:10.1242/jcs.144550

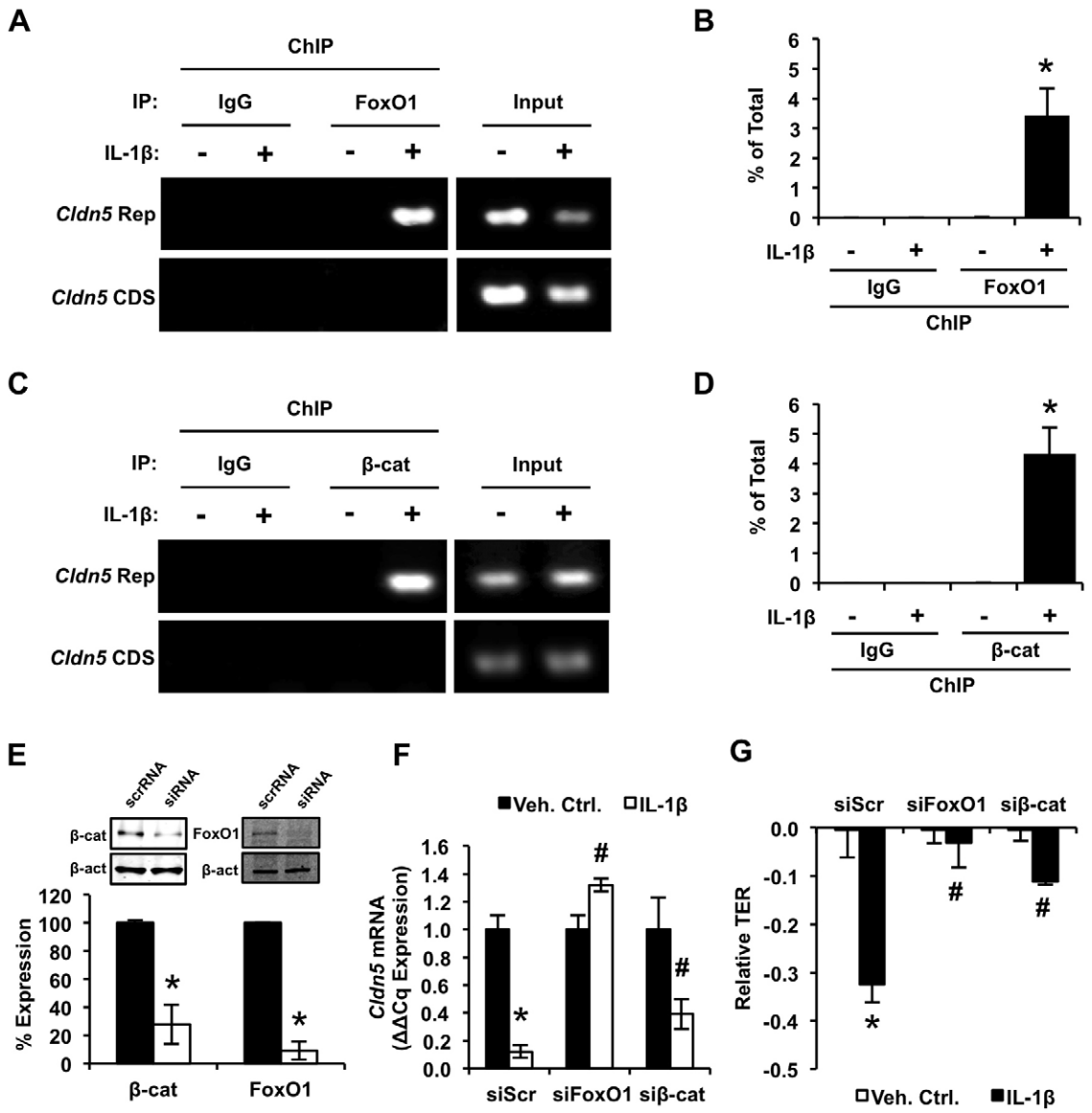

Fig. 6. IL-1β requires the recruitment of FoxO1 and β-catenin to the *Cldn5* repressor to reduce Cldn5 expression. 1.5 hours after treating bEnd.3 cells with IL-1β (100 ng/ml) or vehicle control, bound chromatin was immunoprecipitated (ChIP) with anti-FoxO1, anti-β-catenin or IgG isotype-control antibodies. ChIP samples were assayed by using PCR with primers for the putative *Cldn5* repressor region, whereas primers for the *Cldn5* coding sequence (CDS) were used as negative controls for non-specific DNA precipitation. (A,C) Qualitative PCR results from ChIP assays. (B,D) Quantitative RT-PCR results from ChIP assays. ΔCq (or percentage of total) for the *Cldn5* repressor was calculated by normalizing to input. (E) Western blotting confirmation and quantification of gene knockdown using targeted siRNA against β-catenin (siβ-cat), FoxO1 (siFoxO1) or scrambled control (siScr). FoxO1 and β-catenin knockdown attenuated IL-1β-induced downregulation of *Cldn5* mRNA at 1.5 hours after treatment (F) and barrier dysfunction at 24 hours (G). Data represent the mean±s.e.m. **P*<0.05 compared with control, $^{\#}P$<0.05 compared with siScr treated with IL-1β; Student's *t*-test.

nmMlck deficiency in BMVECs completely abolished IL-1β-mediated barrier dysfunction. Furthermore, the ectopic expression of nmMlck in *nmmlck*$^{-/-}$ BMVECs reverted the attenuation of IL-1β-mediated barrier dysfunction (Fig. 8C). Consistent with the evidence that the activation of β-catenin is dependent on nmMlck, the ectopic expression of active β-catenin in *nmmlck*$^{-/-}$ BMVECs also restored IL-1β-mediated barrier dysfunction (Fig. 8D). These results suggest that nmMlck is required for IL-1β-mediated downregulation of Cldn5 in BMVECs.

DISCUSSION

In this study, we report newly identified molecular details underlying some of the effects of aberrant IL-1β signaling in brain microvascular endothelium. First, we demonstrate that, in our model, IL-1β induced size-selective hyperpermeability in BMVEC monolayers, with a concomitant decrease in Cldn5 expression. After determining that the IL-1β-mediated decrease in Cldn5 protein expression was preceded by downregulation of *Cldn5* mRNA, we determined that IL-1β-induced Cldn5 changes are mediated by FoxO1- and β-catenin-dependent repression of transcription from the *Cldn5* gene. Most importantly, we discovered that nmMlck is a kinase that is essential for transducing IL-1β stimulation, which ultimately leads to Cldn5 downregulation and BMVEC barrier dysfunction. Furthermore, our data indicate that the nuclear translocation of β-catenin and FoxO1 in response to IL-1β is a result of independent

Journal of Cell Science (2014) 127, 1840–1853 doi:10.1242/jcs.144550

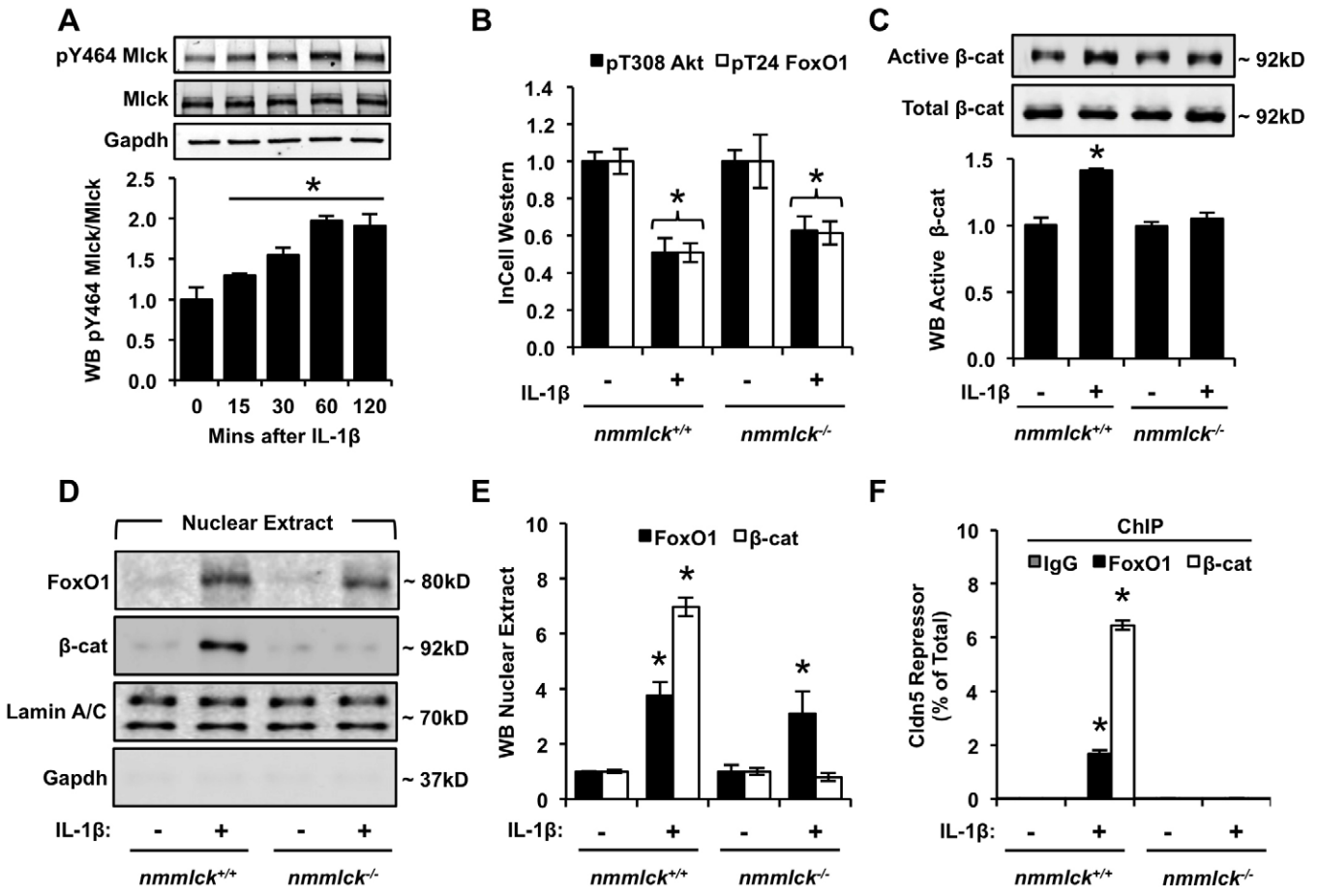

Fig. 7. nmMlck is required for β-catenin and FoxO1 occupancy of the *Cldn5* repressor. Primary BMVECs were isolated from cortices of wild-type (*nmmlck*$^{+/+}$) and nmMlck homozygous knockout (*nmmlck*$^{-/-}$) mice. (A) Treating BMVECs with IL-1β (100 ng/ml) acutely (within 15 minutes) activated nmMlck, as indicated by increased phosphorylation of Y464 in a time-dependent manner. (B) ICWs were used to assess IL-1β-mediated inactivation of the Akt–FoxO1 pathway in BMVECs, by using phosphospecific antibodies against T308 on Akt (pT308 Akt) and T24 on FoxO1 (pT24 FoxO1). Antibodies against total Akt and FoxO1 were used for co-labeling, and the measurements were used to normalize phosphospecific signals. (C) IL-1β (100 ng/ml, 1.5 hours) increased the ratio of active β-catenin (hypophosphorylated at GSK3β sites Ser37 and Thr41) to total β-catenin in BMVECs isolated from *nmmlck*$^{+/+}$ mice, but not in those isolated from *nmmlck*$^{-/-}$ mice. **P*<0.05 compared with control. (D,E) Consistent with the inactivation and activation signals on Akt, FoxO1 and β-catenin, nmMlck deficiency attenuated IL-1β-mediated nuclear accumulation of β-catenin, but not nuclear accumulation of FoxO1. (F) Although IL-1β treatment led to nuclear accumulation of FoxO1 in both *nmmlck*$^{+/+}$ and *nmmlck*$^{-/-}$ BMVECs, the absence of β-catenin in the nuclei of *nmmlck*$^{-/-}$ BMVECs treated with IL-1β prevented the binding of FoxO1 to the *Cldn5* repressor. Data represent the mean±s.e.m. **P*<0.05 compared with all other groups; Student's *t*-test.

intracellular trafficking mechanisms that converge in the nucleus, when both proteins bind to the putative *Cldn5* repressor. Moreover, we demonstrate that nmMlck acts upstream of β-catenin activation and nuclear translocation, yet is not involved in Akt inactivation and FoxO1 nuclear accumulation. However, most notably, our work shows that a lack of nmMlck-induced β-catenin nuclear translocation is sufficient to abrogate IL-1β-induced Cldn5 repression.

Current evidence indicates that endothelial hyperpermeability responses to various stimuli differ in terms of their timing (onset and duration) and in terms of the charge and size of molecules that move across endothelial barriers in different vascular beds (Michel and Curry, 1999; Bazzoni and Dejana, 2004). For example, vascular endothelial growth factor (VEGF) is known to induce a biphasic hyperpermeability response – an initial response lasting just a few minutes and a longer sustained response lasting for many hours (Bates, 2010). Cohen et al. demonstrated that treating bovine pulmonary artery endothelial cells with VEGF induced a delayed and prolonged (6–48 hours) response that only increased the permeability coefficient of molecules with a molecular radius smaller than ~60 Å (Cohen et al., 1999). In the same studies, thrombin-induced hyperpermeability was found to be more transient (5–90 minutes), and treatment with thrombin induced hyperpermeability to solutes with a molecular radius that was larger than ~60 Å. Other cytokines, such as TNF-α and IL-1α, also induce prolonged hyperpermeability, which lasts for 12–48 hours in bovine aortic endothelial cells (Royall et al., 1989). Our data for IL-1β-mediated BMVEC dysfunction seems to be consistent with permeability-inducing factors that induce longer sustained responses and only increase monolayer hyperpermeability to small molecules. However, it is of note that IL-1β has been shown to induce albumin hyperpermeability in non-brain derived endothelial cell monolayers (Ganter et al., 2008; Puhlmann et al., 2005). Our data are also consistent with hyperpermeability mediated by the loss of Cldn5 in the BBB. Using Cldn5-null mice, Nitta et al. performed a series of BBB permeability assays with tracers of different molecular masses to determine the effect of Cldn5 loss on the BBB (Nitta et al., 2003). They discovered that the

Journal of Cell Science (2014) 127, 1840–1853 doi:10.1242/jcs.144550

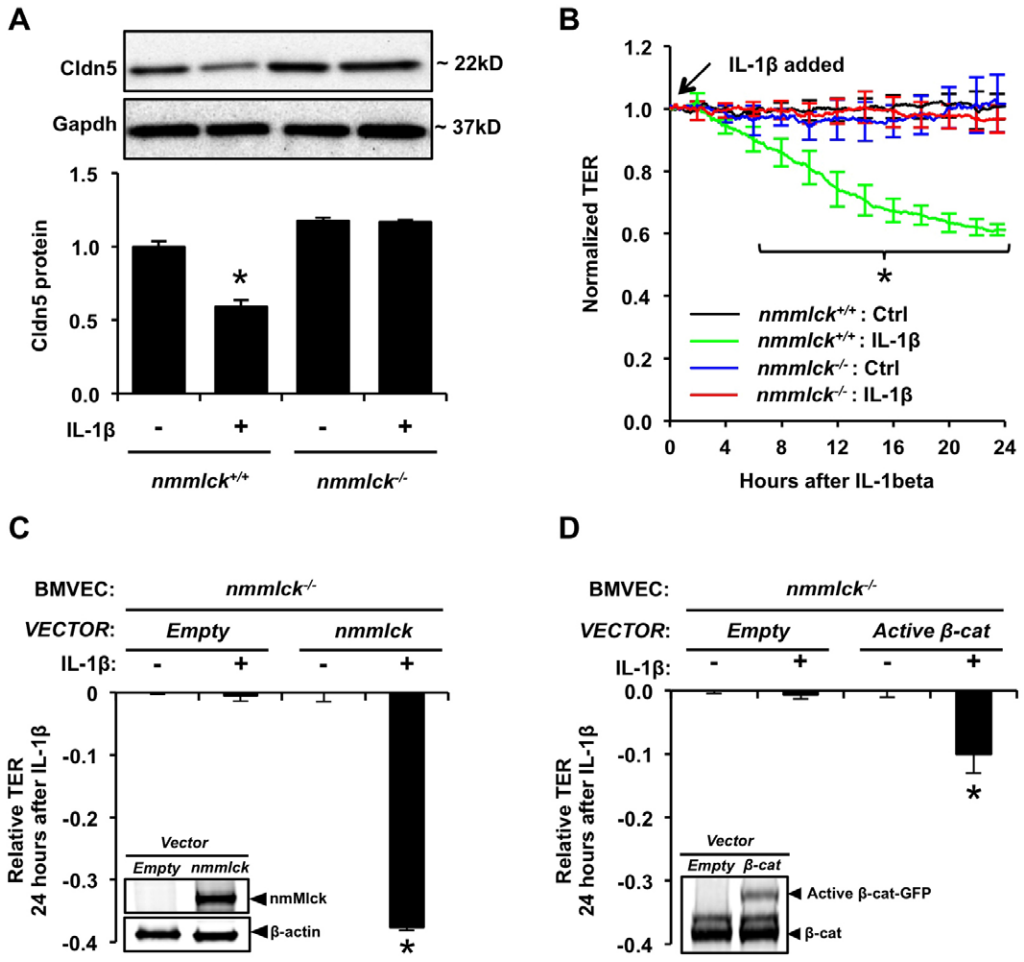

Fig. 8. nmMlck deficiency attenuates IL-1β-mediated dysfunction of the brain endothelial barrier and Cldn5 downregulation. (A) Western blotting for Cldn5 in lysates from BMVECs treated with IL-1β (100 ng/ml, 24 hours) revealed that IL-1β-mediated Cldn5 downregulation is dependent on nmMlck. (B) ECIS experiments demonstrated that BMVECs from *nmmlck*$^{+/+}$ mice respond to IL-1β in a similar fashion to bEnd.3 cells. (C) Ectopic expression of nmMlck in *nmmlck*$^{-/-}$ BMVECs reverts the attenuation of IL-1β-mediated barrier dysfunction. (D) Consistent with the evidence that activation of β-catenin is dependent on nmMlck, ectopic expression of active β-catenin in *nmmlck*$^{-/-}$ BMVECs also restores IL-1β-mediated barrier dysfunction. Data represent the mean±s.e.m. *P<0.05 compared with all other groups; Student's *t*-test.

BBB of Cldn5-deficient mice was more permeable to molecules of less than ~0.8–10 kDa compared with wild-type mice, and histological analysis failed to demonstrate extravasation of endogenous albumin. Our data are similar, in that IL-1β- or siRNA-mediated reduction in Cldn5 levels in BMVECs induced size-selective hyperpermeability to molecules of 0.8–4.4 kDa, but not to albumin.

Tight junctions, rather than being merely static barriers, have recently been discovered to have a highly fluidic and dynamic nature. Studies using fluorescence recovery after photobleaching (FRAP) analysis have found that the turnover of proteins in tight junction strands is much shorter than previously thought (Shen et al., 2008). It has been reported that Cldn5 has a relatively short half-life and can be polyubiquitylated in the membrane, tagging it for degradation (Mandel et al., 2012). The role that this process plays in inflammatory pathogenesis has yet to be determined. Here, we report that IL-1β mediates the loss of Cldn5 protein from BMVECs, and that this loss is correlated with IL-1β-mediated hyperpermeability. Furthermore, we identify that IL-1β triggers the downregulation of *Cldn5* mRNA, which precedes the onset of IL-1β-mediated loss of Cldn5 protein. Accordingly, we sought to determine a mechanism that would explain the gene regulatory response that was observed. It is known that elevated levels of plasma homocysteine cause a decrease in Cldn5 expression in BMVECs, through a mechanism involving the nuclear translocation of β-catenin and the binding of this protein to the putative *Cldn5* repressor (Beard et al., 2011). This mechanism has also been reported in LMVECs in response to acrolein-induced lung injury (Jang et al., 2011). Furthermore, IL-1β has been shown to act in conjunction with tobacco smoke in mouse cardiac endothelial cells to induce the disassembly of the adherens junction complexes and the subsequent translocation of β-catenin to the nucleus (Barbieri et al., 2008; Barbieri and Weksler, 2007). Although these studies did not directly examine Cldn5 as an affected end point, they led us to explore the spatial regulation of β-catenin during IL-1β-mediated downregulation of Cldn5 in BMVECs. Indeed, we discovered that the IL-1β-mediated loss of *Cldn5* mRNA in BMVECs was dependent on both β-catenin and FoxO1, and concomitantly was associated with: (1) the inactivation of Akt and resulting nuclear translocation of FoxO1; (2) the activation and nuclear translocation of β-catenin; and (3) the binding of both FoxO1 and β-catenin to the *Cldn5* repressor.

In addition to its role in stabilizing the adherens junction, β-catenin is also well known to play a role in regulating transcription downstream of Wnt signaling during the development of the BBB. Daneman et al. described an essential role for Wnt–β-catenin signaling in driving the development of the BBB (Daneman et al., 2009). Dejana and colleagues recently reported that treatment of BMVECs *in vitro* with either Wnt3a or inhibitors of Gsk-3β resulted in β-catenin nuclear accumulation that was accompanied by an increase in Cldn3 expression and increased barrier tightness (Liebner et al., 2008; Paolinelli et al.,

2013). Given the conflicting effects of β-catenin nuclear translocation on barrier loosening or barrier tightening, we evaluated mRNA from IL-1β-treated BMVECs using a PCR array for tight junction genes, and compared the results with those reported for BMVECs treated with Wnt3a. Our results indicated a different expression profile associated with β-catenin transcription than that reported to result from Wnt3a treatment (Liebner et al., 2008). Namely, we demonstrate that IL-1β-mediated nuclear translocation of β-catenin was associated with an increase in the expression of *Cldn1* and a decrease in *Cldn5* and *Ocln*, whereas Wnt3a-mediated β-catenin nuclear translocation was associated with an increase in *Cldn3*, but no change in *Cldn1*, *Cldn5* or *Ocln* expression. Consistent with other studies demonstrating that pathologic stimuli increase the nuclear accumulation of β-catenin in association with barrier dysfunction, we conclude that β-catenin transcriptional activity is context specific (differing in developmental versus pathologic contexts) and might depend on the activation or inactivation of other signaling pathways. Our studies indicate that one such pathway is the simultaneous inactivation of Akt and increased FoxO1 activity.

Here, we demonstrate for the first time that nmMlck modulates IL-1β-induced barrier dysfunction in BMVECs. Our finding of nmMlck-dependent β-catenin dissociation from adherens junctions, concomitant with β-catenin activation, is consistent with previous reports describing a role for nmMlck in modulating inflammatory-mediated permeability (Shen et al., 2010). There is increasing evidence that nmMlck serves as a convergent kinase that mediates endothelial barrier dysfunction in response to multiple inflammatory-inducing agents (Shen et al., 2010). In the past, the role of nmMlck in endothelial hyperpermeability has been attributed to its ability to mediate the activation of the cytoskeletal motor machinery, which produces contractile force that counteracts cell–cell adhesion, producing widened intercellular junctions (Yuan and Rigor, 2010). The uncoupling of adherens junctions in inflammatory conditions is often reported to occur simultaneously with actinomyosin contractility in endothelium, and nmMlck inhibition or deficiency is reported to rescue both. This has prompted a hypothesis that nmMlck phosphorylates signaling or regulatory proteins other than MLC. Although β-catenin activation and dissociation from adherens junctions seems to be dependent on nmMlck, future work is still needed to elucidate the exact molecular mechanisms by which nmMlck transduces this signal. Src-mediated phosphorylation of β-catenin and/or VE-cadherin has been shown to be an important signaling event leading to adherens junction uncoupling (Cohen et al., 1999; Dejana et al., 2008; McEwen et al., 2012). We recently reported that Src-activation in response to thrombin was dependent on the presence of nmMlck (Sun et al., 2011), suggesting that nmMlck could be upstream of Src-mediated tyrosine phosphorylation of the adherens junction and subsequent uncoupling. However, it is also thought that β-catenin that is dissociated from the adherens junction needs to be phosphorylated at serine residues in order to be stable in the cytoplasm (Daugherty and Gottardi, 2007). Both serine/threonine kinases PKA (Hino et al., 2005) and Akt (Fang et al., 2007) have been shown to mediate β-catenin stabilization in certain models. Our data support the possibility that nmMlck serves as a serine/threonine kinase, catalyzing β-catenin phosphorylation and thereby stabilizing the protein so that it can be translocated to the nucleus.

In conclusion, this study demonstrates that nmMlck modulates IL-1β-mediated barrier dysfunction in BMVECs by a mechanism that involves the activation of β-catenin, its dissociation from junctions, nuclear translocation and subsequent transcriptional repression of *Cldn5*. This work has shed light on previously unknown effects of IL-1β-mediated barrier dysfunction and nmMlck-dependent processes in BMVECs. Given the finding that nmMlck is expendable under normal physiological conditions, but is essential in transducing the pro-inflammatory signal of IL-1β in BMVECs, therapeutic targeting of this isoform might prove effective in treating BBB hyperpermeability in neuroinflammatory diseases.

MATERIALS AND METHODS

All animal use was approved by the University of South Florida Health Institutional Animal Care and Use Committee and performed in accordance with the Guide for the Care and Use of Laboratory Animals. All recombinant IL-1β used in these experiments was purchased from Reprokine (Rehovot, Israel), reconstituted in PBS plus 0.1% bovine serum albumin (BSA), sterile-filtered, aliquoted and frozen once before use.

BMVEC culture

Two models of BMVECs were used in these studies: (1) immortalized murine BMVECs, or bEnd.3 cells (ATCC, VA, USA), and (2) primary BMVECs isolated from mice with homozygous deletion of nmMlck (*nmmlck*$^{-/-}$) or wild-type littermates (*nmmlck*$^{+/+}$). The mice used in these studies were obtained and maintained as described previously (Sun et al., 2011; Tinsley et al., 2004; Wainwright et al., 2003). The bEnd.3 cells were purchased from ATCC and cultured in the recommended medium. All experiments were performed with bEnd.3 cells from the third to sixth passages. Primary BMVECs were isolated as described previously, with some modifications (Stamatovic et al., 2005). Briefly, cortices from mice were harvested, placed in DMEM with 2% bovine calf serum (BCS) (DMEM-S), and dispersed. Suspensions were mixed in DMEM-S/dextran (~70 kDa; Sigma, MO) to bring the final concentration of dextran to 18%, and were then centrifuged for 10 minutes at 10,000 ***g***. The microvessel-containing pellet was rinsed twice in DMEM-S, resuspended and passed through a 100-µm cell strainer. The flow-through was passed through a 40-µm cell strainer to retain the microvessels. The microvessels were washed and resuspended in HBSS [1 mg/ml collagenase/dispase (Roche, IN), 10 U/µl DNAase I (New England Biolabs, MA) and 1 µg/ml N_{α}-tosyl-L-lysine chloromethyl ketone (TLCK; Sigma, MO)] for 40 minutes at 37℃. BMVECs were cultured in endothelial growth medium (Cell Biologics, IL) and grown on culture plates pre-coated with collagen type IV (BD Biosciences, CA). Only initially plated cells or cells passaged once at a 1:2 ratio were used in these experiments. All BMVECs were cultured at 37℃ in a humidified incubator under 5% CO_2. Before use in experiments, cells were grown for 5 days post-confluence to ensure the maturation of the endothelium and development of tight junctions.

Transendothelial electrical resistance

BMVEC barrier function was determined as described previously (Yuan and Rigor, 2010), by measuring the cell–cell adhesive resistance to electric current using an electric cell–substrate impedance sensing (ECIS) system (Applied Biophysics, Troy, NY). Briefly, 2×10^5 endothelial cells were seeded onto ECIS electrode arrays pre-coated with collagen IV. After culture for 5 days post-confluence, the arrays were attached to the ECIS system. Using a 1-V, 4000-Hz alternating-current signal supplied through a 1-MΩ resistor to a constant-current source, in-phase voltage and out-of-phase voltage were recorded with ECMS 1.0 software (CET, IA). ECIS tracings are expressed as transendothelial electric resistance (TER) and are normalized to the baseline. The time when IL-1β (100 or 200 ng/ml) or vehicle control (0.1% BSA in PBS) was added is set to zero. TER changes were recorded and submitted for statistical analyses at specified time-points ($n=3$; for three independent experiments).

Transwell permeability assays

For transwell permeability assays, 2×10^5 BMVECs were seeded in the upper 'apical' chamber of 0.4-µm transwell inserts (Corning, MA) that

were coated with collagen IV. After culture for 5 days post-confluence, BMVECs were treated with IL-1β (100 ng/ml), or vehicle control (0.1% BSA in PBS) for the indicated times. At 1 hour prior to the sampling time-point, stock concentrations of molecular tracers were added to the upper chamber to bring the final concentration to 0.5 mg/ml. Samples were collected from both the upper (luminal) and lower (abluminal) chambers for fluorometry analysis. The molecular tracers (Sigma, MO) used in these studies were: (1) sodium fluorescein (376 Da; Stokes' radius≈0.45 nm), (2) tetramethylrhodamine isothiocyanate (TRITC)-conjugated dextran (4.4 kDa; Stokes' radius≈1.4 nm) and (3) fluorescein isothiocyanate (FITC)-conjugated albumin (66.4 kDa; Stokes' radius≈3.48 nm). The concentration of each tracer was determined using a standard curve, and the permeability coefficient was calculated as follows: $P_S=[A]/t\times1/A\times V/[L]$, where $[A]$ is the abluminal concentration, t is time (in seconds), A is the area of the membrane (in cm^2), V is the volume of the abluminal chamber, and $[L]$ is the luminal concentration. P_S ($\times10^{-6}$ cm/s) for each tracer is represented as the mean and s.e.m. from three independent experiments.

Western blot analysis of BMVEC lysates

For Cldn5 analyses, BMVECs were harvested in lysis buffer [PBS pH 7.4, 1% Triton X-100 and complete protease and phosphatase inhibitors (Roche, IN)]. For all other protein analyses, RIPA lysis buffer with complete protease and phosphatase inhibitors was used. The protein concentration of each sample was quantified by using the bicinchoninic acid assay (BCA) and normalized, and samples were then denatured in 4× Laemmli sample buffer (Li-Cor, NE) with 10% β-mercaptoethanol, separated by SDS-PAGE and blotted onto nitrocellulose membrane. Blots were probed with primary antibodies and then with the appropriate secondary antibodies conjugated to infrared dyes, and were analyzed on Odyssey (Li-Cor). Band densitometry was performed with ImageJ software (NIH, MD). Data represents the mean±s.e.m. of densitometry results, normalized to a reference protein, from at least three independent experiments. Antibodies against the following proteins were used for western blotting: Cldn5 (Invitrogen, CA); pT308 Akt, Akt, pT24 FoxO1 and Lamin A/C (Cell Signaling, MA); GAPDH, VE-cadherin and β-catenin (Santa Cruz Biotechnology, CA); active β-catenin (clone 8E7; EMD Millipore, MA).

ICWs and immunocytochemical analyses

BMVECs were grown for 5 days post-confluence on coverslips for immunocytochemistry (ICC) or on 96-well plates for ICW. For both procedures, fixation and immunolabeling were performed in the same way and according to standard protocols. Briefly, after respective treatments, BMVECs were washed twice (in PBS with 2 mM $CaCl_2$ and 2 mM $MgCl_2$). The PBS was removed and cells were incubated in 4% paraformaldehyde (PFA) in PBS for 10 minutes, rinsed twice in PBS, permeabilized (in PBS plus 0.1% Triton X-100) and blocked (in PBS plus 3% BSA and 0.01% Tween-20) for 2 hours at room temperature. The samples were incubated with primary antibodies (diluted 1:50 in PBS plus 0.01% Tween-20 and 3% BSA) overnight at 4℃, washed three times for 10 minutes each (in PBS plus 0.1% Tween-20) and incubated with appropriate secondary antibody (diluted 1:200 in PBS plus 0.01% Tween-20 and 2% BSA). Secondary antibodies were Alexa Fluor conjugated (Invitrogen) for ICC and IRDye conjugated (Li-Cor) for ICWs. Immunofluorescence confocal microscopy was performed with an Olympus FV1000 MPE multiphoton laser scanning microscope (Olympus), and the images were analyzed with ImageJ software (NIH, MD). For ICW, 96-well plates were scanned and analyzed with the Odyssey CLX (Li-Cor, NE). All primary antibodies used for ICC and ICW were the same as those used for western blotting. ICC images were obtained from three independent experiments and representative confocal micrograph image stacks are presented. Samples stained with secondary antibodies only were used as ICC background controls (data not shown). For ICW data, secondary-only background fluorescence was subtracted, relative absorbance was normalized to treatment control or time-point zero, and the data are represented as the mean±s.e.m. from three independent experiments.

RNA preparation and quantitative RT-PCR

After respective treatments, total RNA from BMVEC monolayers was harvested and prepared by using the Aurum Total RNA Extraction Kit (Bio-Rad, CA). RNA was reverse-transcribed using the iScript cDNA Synthesis Kit (Bio-Rad, CA), using 1 µg of total RNA per 20-µl reaction. Validated primers (PrimePCR Assays; Bio-Rad, CA) for the genes and reference genes that were quantified in these studies were used in either individual assays or as custom-designed PCR Arrays (PrimePCR Arrays; Bio-Rad, CA). *G6pdx* and *Actb* were used as reference genes. For real-time PCR reactions, SsoAdvanced SYBR Green Supermix was used, and RT-PCR was run and analyzed on Bio-Rad CFX Connect (Bio-Rad, CA) as per the manufacturer's instructions.

High-salt nuclear extraction

Protein from nuclear extracts was obtained as described previously (Lin et al., 2001). Briefly, after treatment, cells were scraped and collected in non-nuclear extraction buffer and left on ice for 10 minutes. Lysates were centrifuged at 845 ***g*** for 10 minutes at 4℃, and the supernatants were removed. The remaining pellet of nuclei was washed three times with 500 µl of non-nuclear extraction buffer, before resuspending in high-salt nuclear extraction buffer. Lysates were homogenized with 20 full strokes in a Dounce homogenizer and were then incubated on ice for 30 minutes. The suspension was then centrifuged at 24,000 ***g*** for 20 minutes at 4℃. Supernatants were collected as the nuclear extract. Protein was quantified by using the BCA assay (Fisher Scientific, USA), normalized to total protein in 4× Laemmli sample buffer, and then used in western blotting. Western blots of nuclear extracts were immunolabeled with antibodies against FoxO1 and β-catenin, then stripped and reprobed for Lamin A/C as a loading control and for Gapdh to insure successful nuclear fractionation.

ChIP assay

ChIP assays were performed on chromatin from treated BMVECs as described previously, with minor modifications (Taddei et al., 2008). Briefly, cells were cross-linked with 1% PFA. PFA was then quenched, and the cells were scraped and resuspended in sonication buffer and sonicated until DNA reached an average size of 500 bp. After fragmentation, 200 µg of DNA was incubated with 5 µg of antibody with rotation overnight at 4℃. Conjugates were precipitated by using protein-G–agarose beads and blocked (Fisher Scientific). Precipitates were incubated with proteinase K (New England Biolabs, MA). DNA was precipitated according to standard procedures and was amplified in standard qualitative PCR and qRT-PCR reactions using oligonucleotides flanking the putative *Cldn5* repressor region. Non-precipitated or input samples were used as positive controls and oligonucleotides flanking Cldn5-coding DNA were used as exclusion controls. ΔCq was calculated by normalizing to input.

Gene knockdown and transfer

Silencing of Cldn5, β-catenin or FoxO1 was achieved by using targeted siRNA duplexes purchased from Santa Cruz Biotechnology (CA) (sc-43045, sc-29210 and sc-35383, respectively). Ectopic expression of nmMlck was achieved by using an untagged plasmid (pCMV6 vector) containing the full-length cDNA for the mouse *Mylk* gene (Origene Technologies, MD). Ectopic expression of transcriptionally active β-catenin (Wrobel et al., 2007) was achieved by using a plasmid (pCAG-GFP vector) containing a mutated *Ctnnb1* gene (encoding a protein with a deletion of the first 90 amino acids of β-catenin, Addgene plasmid 26645; Addgene, MA). The introduction of siRNA duplexes and plasmids was achieved using the Nucleofector kit (Amaxa Biosystems, MD). Transfection was performed according to the manufacturer's instructions with minor modifications. Briefly, 5×10^5 BMVECs were resuspended in 100 µl of Nucleofector solution, mixed with 2 µg of siRNA or DNA and transfected with program T-011 on the Lonza Nucleofector device. Cells were then plated onto gelatin-coated ECIS arrays or culture flasks. Scrambled siRNA or empty vectors were used as controls. Knockdown and expression were determined by western blotting.

Statistics

The data are presented as the mean±s.e.m. (*n* is the number of animals or cell assays from at least three independent experiments). Pair-wise comparisons were made by using Student's *t*-test, and group-wise data were compared by analysis of variance with Tukey or Dunnett post hoc analyses; α was set at 0.05 *a priori* for statistical significance.

Acknowledgements

We thank Jonathan Overstreet for his excellent technical assistance in the laboratory. We also thank the USF Health Lisa Muma Weitz Laboratory for Advanced Microscopy and Cell Imaging and the staff for excellent technical assistance in obtaining microscopy images.

Competing interests

The authors declare no competing interests.

Author contributions

This study was conceived and designed by R.S.B.J. and S.Y.Y. Experiments were designed, executed and interpreted by all listed authors. The manuscript was prepared by R.S.B.J., R.J.H. and S.Y.Y.

Funding

This work was supported in part by the National Institutes of Health Research Project Grants [grant numbers GM097270, HL070752, HL096640 and HL061507]. Deposited in PMC for release after 12 months.

Supplementary material

Supplementary material available online at
http://jcs.biologists.org/lookup/suppl/doi:10.1242/jcs.144550/-/DC1

References

Banks, W. A. (1999). Physiology and pathology of the blood–brain barrier: implications for microbial pathogenesis, drug delivery and neurodegenerative disorders. *J. Neurovirol.* **5**, 538-555.

Barbieri, S. S. and Weksler, B. B. (2007). Tobacco smoke cooperates with interleukin-1beta to alter beta-catenin trafficking in vascular endothelium resulting in increased permeability and induction of cyclooxygenase-2 expression in vitro and in vivo. *FASEB J.* **21**, 1831-1843.

Barbieri, S. S., Ruggiero, L., Tremoli, E. and Weksler, B. B. (2008). Suppressing PTEN activity by tobacco smoke plus interleukin-1beta modulates dissociation of VE-cadherin/beta-catenin complexes in endothelium. *Arterioscler. Thromb. Vasc. Biol.* **28**, 732-738.

Basu, A., Krady, J. K. and Levison, S. W. (2004). Interleukin-1: a master regulator of neuroinflammation. *J. Neurosci. Res.* **78**, 151-156.

Bates, D. O. (2010). Vascular endothelial growth factors and vascular permeability. *Cardiovasc. Res.* **87**, 262-271.

Bazzoni, G. and Dejana, E. (2004). Endothelial cell-to-cell junctions: molecular organization and role in vascular homeostasis. *Physiol. Rev.* **84**, 869-901.

Beard, R. S., Jr, Reynolds, J. J. and Bearden, S. E. (2011). Hyperhomocysteinemia increases permeability of the blood-brain barrier by NMDA receptor-dependent regulation of adherens and tight junctions. *Blood* **118**, 2007-2014.

Blamire, A. M., Anthony, D. C., Rajagopalan, B., Sibson, N. R., Perry, V. H. and Styles, P. (2000). Interleukin-1beta -induced changes in blood-brain barrier permeability, apparent diffusion coefficient, and cerebral blood volume in the rat brain: a magnetic resonance study. *J. Neurosci.* **20**, 8153-8159.

Chakraborty, S., Kaushik, D. K., Gupta, M. and Basu, A. (2010). Inflammasome signaling at the heart of central nervous system pathology. *J. Neurosci. Res.* **88**, 1615-1631.

Cohen, A. W., Carbajal, J. M. and Schaeffer, R. C., Jr (1999). VEGF stimulates tyrosine phosphorylation of beta-catenin and small-pore endothelial barrier dysfunction. *Am. J. Physiol.* **277**, H2038-H2049.

Daneman, R., Agalliu, D., Zhou, L., Kuhnert, F., Kuo, C. J. and Barres, B. A. (2009). Wnt/beta-catenin signaling is required for CNS, but not non-CNS, angiogenesis. *Proc. Natl. Acad. Sci. USA* **106**, 641-646.

Daneman, R., Zhou, L., Agalliu, D., Cahoy, J. D., Kaushal, A. and Barres, B. A. (2010). The mouse blood-brain barrier transcriptome: a new resource for understanding the development and function of brain endothelial cells. *PLoS ONE* **5**, e13741.

Daugherty, R. L. and Gottardi, C. J. (2007). Phospho-regulation of Beta-catenin adhesion and signaling functions. *Physiology (Bethesda)* **22**, 303-309.

Dejana, E. (2004). Endothelial cell-cell junctions: happy together. *Nat. Rev. Mol. Cell Biol.* **5**, 261-270.

Dejana, E., Orsenigo, F. and Lampugnani, M. G. (2008). The role of adherens junctions and VE-cadherin in the control of vascular permeability. *J. Cell Sci.* **121**, 2115-2122.

Didier, N., Romero, I. A., Créminon, C., Wijkhuisen, A., Grassi, J. and Mabondzo, A. (2003). Secretion of interleukin-1beta by astrocytes mediates endothelin-1 and tumour necrosis factor-alpha effects on human brain microvascular endothelial cell permeability. *J. Neurochem.* **86**, 246-254.

Fang, D., Hawke, D., Zheng, Y., Xia, Y., Meisenhelder, J., Nika, H., Mills, G. B., Kobayashi, R., Hunter, T. and Lu, Z. (2007). Phosphorylation of beta-catenin by AKT promotes beta-catenin transcriptional activity. *J. Biol. Chem.* **282**, 11221-11229.

Ganter, M. T., Roux, J., Miyazawa, B., Howard, M., Frank, J. A., Su, G., Sheppard, D., Violette, S. M., Weinreb, P. H., Horan, G. S. et al. (2008). Interleukin-1beta causes acute lung injury via alphavbeta5 and alphavbeta6 integrin-dependent mechanisms. *Circ. Res.* **102**, 804-812.

Hawkins, B. T. and Davis, T. P. (2005). The blood-brain barrier/neurovascular unit in health and disease. *Pharmacol. Rev.* **57**, 173-185.

Hino, S., Tanji, C., Nakayama, K. I. and Kikuchi, A. (2005). Phosphorylation of beta-catenin by cyclic AMP-dependent protein kinase stabilizes beta-catenin through inhibition of its ubiquitination. *Mol. Cell. Biol.* **25**, 9063-9072.

Jang, A. S., Concel, V. J., Bein, K., Brant, K. A., Liu, S., Pope-Varsalona, H., Dopico, R. A., Jr, Di, Y. P., Knoell, D. L., Barchowsky, A. et al. (2011). Endothelial dysfunction and claudin 5 regulation during acrolein-induced lung injury. *Am. J. Respir. Cell Mol. Biol.* **44**, 483-490.

Lazovic, J., Basu, A., Lin, H. W., Rothstein, R. P., Krady, J. K., Smith, M. B. and Levison, S. W. (2005). Neuroinflammation and both cytotoxic and vasogenic edema are reduced in interleukin-1 type 1 receptor-deficient mice conferring neuroprotection. *Stroke* **36**, 2226-2231.

Liebner, S., Corada, M., Bangsow, T., Babbage, J., Taddei, A., Czupalla, C. J., Reis, M., Felici, A., Wolburg, H., Fruttiger, M. et al. (2008). Wnt/beta-catenin signaling controls development of the blood-brain barrier. *J. Cell Biol.* **183**, 409-417.

Ligumsky, M., Simon, P. L., Karmeli, F. and Rachmilewitz, D. (1990). Role of interleukin 1 in inflammatory bowel disease—enhanced production during active disease. *Gut* **31**, 686-689.

Lin, S. Y., Makino, K., Xia, W., Matin, A., Wen, Y., Kwong, K. Y., Bourguignon, L. and Hung, M. C. (2001). Nuclear localization of EGF receptor and its potential new role as a transcription factor. *Nat. Cell Biol.* **3**, 802-808.

Ma, T. Y., Boivin, M. A., Ye, D., Pedram, A. and Said, H. M. (2005). Mechanism of TNF-alpha modulation of Caco-2 intestinal epithelial tight junction barrier: role of myosin light-chain kinase protein expression. *Am. J. Physiol.* **288**, G422-G430.

Mandel, I., Paperna, T., Volkowich, A., Merhav, M., Glass-Marmor, L. and Miller, A. (2012). The ubiquitin-proteasome pathway regulates claudin 5 degradation. *J. Cell. Biochem.* **113**, 2415-2423.

McColl, B. W., Rothwell, N. J. and Allan, S. M. (2008). Systemic inflammation alters the kinetics of cerebrovascular tight junction disruption after experimental stroke in mice. *J. Neurosci.* **28**, 9451-9462.

McEwen, A. E., Escobar, D. E. and Gottardi, C. J. (2012). Signaling from the adherens junction. *Subcell. Biochem.* **60**, 171-196.

Mehta, D. and Malik, A. B. (2006). Signaling mechanisms regulating endothelial permeability. *Physiol. Rev.* **86**, 279-367.

Michel, C. C. and Curry, F. E. (1999). Microvascular permeability. *Physiol. Rev.* **79**, 703-761.

Miller, D. S. (2010). Regulation of P-glycoprotein and other ABC drug transporters at the blood-brain barrier. *Trends Pharmacol. Sci.* **31**, 246-254.

Nitta, T., Hata, M., Gotoh, S., Seo, Y., Sasaki, H., Hashimoto, N., Furuse, M. and Tsukita, S. (2003). Size-selective loosening of the blood-brain barrier in claudin-5-deficient mice. *J. Cell Biol.* **161**, 653-660.

Paolinelli, R., Corada, M., Ferrarini, L., Devraj, K., Artus, C., Czupalla, C. J., Rudini, N., Maddaluno, L., Papa, E., Engelhardt, B. et al. (2013). Wnt activation of immortalized brain endothelial cells as a tool for generating a standardized model of the blood brain barrier in vitro. *PLoS ONE* **8**, e70233.

Puhlmann, M., Weinreich, D. M., Farma, J. M., Carroll, N. M., Turner, E. M. and Alexander, H. R., Jr (2005). Interleukin-1beta induced vascular permeability is dependent on induction of endothelial tissue factor (TF) activity. *J. Transl. Med.* **3**, 37.

Quagliarello, V. J., Wispelwey, B., Long, W. J., Jr and Scheld, W. M. (1991). Recombinant human interleukin-1 induces meningitis and blood-brain barrier injury in the rat. Characterization and comparison with tumor necrosis factor. *J. Clin. Invest.* **87**, 1360-1366.

Ranaivo, H. R., Carusio, N., Wangensteen, R., Ohlmann, P., Loichot, C., Tesse, A., Chalupsky, K., Lobysheva, I., Haiech, J., Watterson, D. M. et al. (2007). Protection against endotoxic shock as a consequence of reduced nitrosative stress in MLCK210-null mice. *Am. J. Pathol.* **170**, 439-446.

Reynoso, R., Perrin, R. M., Breslin, J. W., Daines, D. A., Watson, K. D., Watterson, D. M., Wu, M. H. and Yuan, S. (2007). A role for long chain myosin light chain kinase (MLCK-210) in microvascular hyperpermeability during severe burns. *Shock* **28**, 589-595.

Rigor, R. R., Beard, R. S., Jr, Litovka, O. P. and Yuan, S. Y. (2012). Interleukin-1β-induced barrier dysfunction is signaled through PKC-θ in human brain microvascular endothelium. *Am. J. Physiol.* **302**, C1513-C1522.

Royall, J. A., Berkow, R. L., Beckman, J. S., Cunningham, M. K., Matalon, S. and Freeman, B. A. (1989). Tumor necrosis factor and interleukin 1 alpha increase vascular endothelial permeability. *Am. J. Physiol.* **257**, L399-L410.

Shen, L., Weber, C. R. and Turner, J. R. (2008). The tight junction protein complex undergoes rapid and continuous molecular remodeling at steady state. *J. Cell Biol.* **181**, 683-695.

Shen, Q., Rigor, R. R., Pivetti, C. D., Wu, M. H. and Yuan, S. Y. (2010). Myosin light chain kinase in microvascular endothelial barrier function. *Cardiovasc. Res.* **87**, 272-280.

Simi, A., Tsakiri, N., Wang, P. and Rothwell, N. J. (2007). Interleukin-1 and inflammatory neurodegeneration. *Biochem. Soc. Trans.* **35**, 1122-1126.
Sohet, F. and Daneman, R. (2013). Genetic mouse models to study blood-brain barrier development and function. *Fluids Barriers CNS* **10**, 3.
Stamatovic, S. M., Shakui, P., Keep, R. F., Moore, B. B., Kunkel, S. L., Van Rooijen, N. and Andjelkovic, A. V. (2005). Monocyte chemoattractant protein-1 regulation of blood-brain barrier permeability. *J. Cereb. Blood Flow Metab.* **25**, 593-606.
Sun, C., Wu, M. H. and Yuan, S. Y. (2011). Nonmuscle myosin light-chain kinase deficiency attenuates atherosclerosis in apolipoprotein E-deficient mice via reduced endothelial barrier dysfunction and monocyte migration. *Circulation* **124**, 48-57.
Taddei, A., Giampietro, C., Conti, A., Orsenigo, F., Breviario, F., Pirazzoli, V., Potente, M., Daly, C., Dimmeler, S. and Dejana, E. (2008). Endothelial adherens junctions control tight junctions by VE-cadherin-mediated upregulation of claudin-5. *Nat. Cell Biol.* **10**, 923-934.
Tinsley, J. H., Yuan, S. Y. and Wilson, E. (2004). Isoform-specific knockout of endothelial myosin light chain kinase: closing the gap on inflammatory lung disease. *Trends Pharmacol. Sci.* **25**, 64-66.
Wainwright, M. S., Rossi, J., Schavocky, J., Crawford, S., Steinhorn, D., Velentza, A. V., Zasadzki, M., Shirinsky, V., Jia, Y., Haiech, J. et al. (2003). Protein kinase involved in lung injury susceptibility: evidence from enzyme isoform genetic knockout and in vivo inhibitor treatment. *Proc. Natl. Acad. Sci. USA* **100**, 6233-6238.
Winter, C. D., Pringle, A. K., Clough, G. F. and Church, M. K. (2004). Raised parenchymal interleukin-6 levels correlate with improved outcome after traumatic brain injury. *Brain* **127**, 315-320.
Wolburg, H., Wolburg-Buchholz, K., Kraus, J., Rascher-Eggstein, G., Liebner, S., Hamm, S., Duffner, F., Grote, E. H., Risau, W. and Engelhardt, B. (2003). Localization of claudin-3 in tight junctions of the blood-brain barrier is selectively lost during experimental autoimmune encephalomyelitis and human glioblastoma multiforme. *Acta Neuropathol.* **105**, 586-592.
Wrobel, C. N., Mutch, C. A., Swaminathan, S., Taketo, M. M. and Chenn, A. (2007). Persistent expression of stabilized beta-catenin delays maturation of radial glial cells into intermediate progenitors. *Dev. Biol.* **309**, 285-297.
Yamasaki, Y., Matsuura, N., Shozuhara, H., Onodera, H., Itoyama, Y. and Kogure, K. (1995). Interleukin-1 as a pathogenetic mediator of ischemic brain damage in rats. *Stroke* **26**, 676-680, discussion 681.
Yuan, S. Y. and Rigor, R. R. (2010). *Regulation of Endothelial Barrier Function*. San Rafael, CA: Morgan & Claypool Life Sciences.
Zlokovic, B. V. (2008). The blood-brain barrier in health and chronic neurodegenerative disorders. *Neuron* **57**, 178-201.